Phase Behavior Modeling of Bitumen and Light Normal Alkanes and CO_2 by PR-EOS and CPA-EOS

Tereza Jindrová, Jiří Mikyška,[*,†] and Abbas Firoozabadi[*,‡]

[†]Faculty of Nuclear Sciences and Physical Engineering, Department of Mathematics, Czech Technical University in Prague, Trojanova 13, 120 00 Prague 2, Czech Republic

[‡]Reservoir Engineering Research Institute (RERI) 595 Lytton Avenue, Suite B, Palo Alto, California 94301, United States

ABSTRACT: The Peng−Robinson (PR) and cubic-plus-association (CPA) equations of state are used to predict the phase behavior and solubility of CO_2 and normal alkanes from C_1 to nC_{10} in several bitumens. Both of the equations of state are investigated over wide ranges of temperature and pressure. The results show that the PR-EOS describes mixure of bitumens with CO_2 and alkanes when there is no second liquid phase or when the asphaltene content in the second liquid phase is not high. The CPA-EOS describes the phase behavior of mixtures of bitumens and CO_2 and alkanes in liquid−liquid states even when the asphaltene content of one of the phases is high. High asphaltene content results in significant association and cross-association where the CPA-EOS is a natural choice. In this work the only adjustable parameter in the CPA-EOS is the cross-association energy parameter, and we show that the solubility of CO_2 and alkanes in bitumens is usually not sensitive to this parameter. However, in two-phase liquid−liquid and three-phase liquid−liquid−vapor states with one phase having a high concentration of asphaltenes, the results become sensitive to the cross-association energy parameter.

1. INTRODUCTION

As the world supply of conventional light crudes decreases, the production from heavy oils and bitumens can supplement the societal energy needs. Knowledge of phase behavior of mixtures of heavy oils and bitumens with various light normal alkanes and CO_2 is important in efficient production from heavy petroleum fluids, especially bitumens. Mixtures of CO_2 and light normal alkanes with bitumen may form vapor−liquid, liquid−liquid, and vapor−liquid−liquid states depending on pressure and temperature conditions. Generally, liquid−liquid states are formed when mixing bitumens with very light alkanes (C_2 to nC_4) at high pressure, while vapor−liquid equilibria are observed at low pressure. Mixing of alkanes such as nC_5 to nC_{10} with bitumens often gives liquid−liquid or vapor−liquid−liquid equilibria. The phase diagrams from X-ray transmission tomography are reported for mixtures of the Athabasca vacuum tower bottoms and *n*-alkanes nC_5, nC_7, nC_{10}, and nC_{12}.[1] Depending on the mixture composition, three- and even four-phase equilibria states are observed.

In the literature, phase behavior predictions of bitumen systems are obtained from different approaches including very detailed characterization and the choice of tuning parameters. One simple modeling approach is based on fugacity−activity coefficients using the equation of state (PR-EOS) and nonrandom two-liquid (NRTL)[2] activity model to calculate the fugacity and activity coefficients in the gas and liquid phases, respectively. This model is used to investigate mixtures of bitumen and light solvents in vapor−liquid equilibrium[3−5] where bitumen is considered as a single component. This approach cannot describe liquid−liquid or vapor−liquid−liquid equilibria.

In most applications, a cubic equation of state such as the PR-EOS or Soave−Redlich−Kwong (SRK) EOS can adequately describe the vapor−liquid equilibria of petroleum fluids over wide range of conditions when mixed with hydrocarbon solvents and CO_2.[4−8] In such systems, the molecular dispersion interactions are dominant. Bitumen consists of various molecules with different hydrocarbon chains and polarities, especially asphaltene molecules which are the most polar, and the most complicated fraction of the crude oil. Asphaltenes give rise to molecular association. In the literature, several ways can be found which have been used to describe normal alkane/bitumen phase behavior. Some of these methods do not account for association explicitly but rather try to tune the EOS parameters or use detailed bitumen characterization to improve the match between experimental data and the model. In refs 6−8, a methodology is developed to characterize bitumen by assessing several extrapolations of the true boiling curve and dividing the extrapolated curve into a number of pseudocomponents (from 16 to 20). In ref 7, phase behavior in vapor−liquid and vapor−liquid−liquid is predicted for the Athabasca vacuum tower bottoms (AVTB) mixed with *n*-decane. Good predictions in vapor−liquid states are obtained, while the second liquid phase cannot be predicted despite detailed characterization of AVTB, use of group contribution methods to estimate the critical properties and boiling points of AVTB, and use of new composite mixing rules for computing covolumes of asymmetric mixtures. To predict the asphaltene precipitation for bitumen/light hydrocarbon and CO_2 mixtures, modifications of the PR-EOS are adopted in refs 6 and 8. The modifcations and adjustments include: (1) volume translation parameters for liquid densities and (2) adjusting the binary interaction parameters set as temperature-dependent,[8] or either constant or defined as a function of critical properties.[6] Despite

these adjustments, the model cannot correctly compute the asphaltene yields from bitumen diluted with n-pentane[8] and n-heptane.[6] When associations become predominant, tuning the parameters of cubic equations or detailed bitumen characterization may not lead to accurate phase behavior predictions.

The incorporation of association in cubic equations of state may lead to more accurate phase behavior predictions. In ref 9 asphaltene precipitation from toluene/n-alkane/bitumen mixtures and from n-alkane/bitumen mixtures is modeled using the PR-EOS. Modifications similar to those in refs 6−8 were used in ref 9; i.e., detailed characterization of bitumen using 30 pseudocomponents, group contribution methods to estimate the critical properties, and tuning of the binary interaction parameters. Further, an average associated molecular weight of asphaltenes is used to incorporate self-association of asphaltenes. The model is applied to higher n-alkanes (from nC_5 to nC_{10}). In the asphaltene precipitation modeling based on liquid−liquid equilibrium, an assumption is made that asphaltenes consitute the precipitated phase without the other hydrocarbons and nonhydrocarbons.

Alternative methods such as the use of the statistical association fluid theory (SAFT) to account for association of complex molecules are explored in refs 10−12. The model based on SAFT is applied to predict the solubility of supercritical CO_2 in the Cold Lake bitumen.[12] According to ref 12, the solubility of CO_2 may be relatively insensitive to asphaltene association; therefore, the SAFT association term is neglected in ref 12. This observation is in line with this work.

The cubic-plus-association equation of state (CPA-EOS) is a simple approach; when there is no need for association incorporation, one reverts back to purely cubic form of the equation of state. The CPA-EOS has been applied to study asphaltene precipitation from heavier n-alkanes (nC_5−nC_7) diluted with model solutions (asphaltene + toluene), heavy oils and bitumens, and live oils, taking into account the self-association between the asphaltene molecules and cross-association between asphaltene and aromatics/resins molecules.[13,14] The CPA-EOS, based on the SRK-EOS for the physical molecular interactions, has been used to predict the solubility of CO_2 in four different bitumens from Alberta reservoirs.[15]

In this work, we apply the CPA-EOS to investigate solubility of light solvents and phase behavior in several bitumens over a wide range of temperature, pressure, and composition to study the effect of association on predictions. The remainder of this paper is organized as follows. Section 2 describes briefly the PR-EOS and CPA-EOS used in this work. Section 3 compares the modeling results with the experimental data in mixtures of CO_2 and n-alkanes (C_1−nC_{10}) and several bitumens. In Section 4, the results are summarized, and the main conclusions are drawn.

2. MODELING AND THEORY

In this work, we model the solubility of CO_2 and n-alkanes (C_1 to nC_{10}) in several bitumens, and partitioning of components between various phases. The precipitants (CO_2 or n-alkanes) are represented as components, but the bitumens are characterized in terms of either three pseudocomponents, i.e., saturates, aromatics/resins, and asphaltenes (the so-called SARA analysis), or several hydrocarbon pseudocomponents (C_1−C_{10}, C_{11}−C_{20}, etc.) and the hydrocarbon residue (C_{n+}) which is further divided into the heavy component and

asphaltenes. The heavy component includes the aromatics and resins or heavy alkanes, aromatics, and resins.

In the PR-EOS, the Helmholtz free energy departure function $A^{\text{departure}}$, based on the Peng−Robinson equation of state (PR-EOS),[16,17] is given by

$$\frac{A_{\text{ph}}^{\text{departure}}}{nRT} = -\ln(1 - bc)$$
$$- \frac{a}{2\sqrt{2}\,bRT}\ln\left(\frac{1 + (1 + \sqrt{2})bc}{1 + (1 - \sqrt{2})bc}\right) \quad (1)$$

where n is the total number of moles, R is the universal gas constant, T is the absolute temperature, c is the molar density of the mixture, and a and b are the energy and volume parameters of the mixture in the PR-EOS given as

$$a = \sum_{i,j} a_{ij}x_ix_j, \quad b = \sum_i b_ix_i, \quad a_{ij} = \sqrt{a_ia_j}\,(1 - k_{ij}) \quad (2)$$

In these equations x_i is the mole fraction of component i, k_{ij} denotes the binary interaction coefficient between component i and j ($k_{ij} = 0$ if $i = j$), and a_i and b_i denote the energy and volume parameters of component i, respectively. The parameters a_i and b_i can be determined from

$$a_i = 0.45724\frac{R^2T_{Ci}^2}{P_{Ci}}[1 + c_i(1 - \sqrt{T_{ri}})]^2,$$
$$b_i = 0.0778\frac{RT_{Ci}}{P_{Ci}} \quad (3)$$

$$c_i = \begin{cases} 0.37464 + 1.54226\omega_i - 0.26992\omega_i^2 & \omega_i \leq 0.5 \\ 0.3796 + 1.485\omega_i - 0.1644\omega_i^2 + 0.01667\omega_i^3 & \omega_i > 0.5 \end{cases}$$

where T_{ri}, T_{Ci}, P_{Ci}, and ω_i denote the reduced temperature, critical temperature, critical pressure, and accentric factor of component i, respectively. In this work, all the binary interaction coefficients k_{ij} are set to zero, except for k_{ij} between CO_2 and C_1 and other components of oil.[18]

In the CPA-EOS,[19] the Helmholtz free energy departure function consists of two parts: the physical part represented by the PR-EOS, which describes the nonassociating molecular interactions such as short-range repulsions and dispersion, and the association part, which is derived from the thermodynamic perturbation theory and describes the polar−polar interactions (self-association and cross-association) of asphaltene and heavy molecules. Assuming that each asphaltene molecule has N_A identical association sites and each heavy molecule has N_R identical cross-association sites, the contribution to the Helmholtz energy departure function due to association can be written as

$$\frac{A_{\text{ass}}^{\text{departure}}}{nRT} = N_Ax_A\left(\ln\chi_A + \frac{1 - \chi_A}{2}\right) +$$
$$N_Rx_R\left(\ln\chi_R + \frac{1 - \chi_R}{2}\right) \quad (4)$$

where the subscripts "A" and "R" stand for asphaltenes and heavy component, respectively, and χ_A and χ_R are the mole fractions of asphaltene and heavy molecules not bonded at one of the association or cross-association sites, respectively. Assuming association bonding between either two asphaltene

molecules or cross-association between asphaltene and heavy molecules and no self-association between heavy molecules, the following simplified expressions can be written

$$\chi_A = \frac{1}{1 + cN_A x_A \chi_A \Delta^{AA} + cN_R x_R \chi_R \Delta^{AR}},$$

$$\chi_R = \frac{1}{1 + cN_A x_A \chi_A \Delta^{AR}} \tag{5}$$

The association strength between molecules i and j is given by

$$\Delta^{ij} = g\kappa_{ij} b_{ij}[\exp(\varepsilon_{ij}/k_B T) - 1], \quad i = A, \quad j = A \text{ or } R$$

where $b_{ij} = (b_i + b_j)/2$, k_B is the Boltzmann constant, ε_{ij} and κ_{ij} are the bonding volume and energy parameters, respectively, and g is the contact value of the radial distribution function of hard-sphere mixture that can be approximated as $g \approx (1 - 0.5\eta)/(1 - \eta)^3$ where $\eta = bc/4$.

3. RESULTS AND DISCUSSION

This work is mainly focused on predicting the solubility and phase behavior of CO_2 and n-alkanes (C_1 to nC_{10}) in several bitumens using the PR-EOS and CPA-EOS and comparing the results with experimental data.[5−8,20−22] As was mentioned above, modifications of the PR-EOS and other cubic equations or using a more detailed bitumen characterization do not provide the description of asphaltene-rich phase in the mixtures of bitumens and normal alkanes such as nC_5, nC_6, and nC_7.

The SARA analysis and compositional data are available for all the petroleum fluids. The key step is the determination of the EOS parameters for pure components and pseudocomponents which include critical temperature T_C, critical pressure P_C, accentric factor ω, molecular weight M_w, and binary interaction coefficients k_{ij} between CO_2 and methane and other components of oil. For pure components, the physical parameters are readily available. For the asphaltene component, the parameters are shown in Table 1. In refs 7 and 8, a higher

Table 1. Parameters of Asphaltenes Used in This Work

	M_w (g/mol)	T_C (K)	P_C (bar)	ω
asphaltenes (in Athabasca vacuum tower bottoms,[7])	3730	1522	6.17	2.0
asphaltenes (in Athabasca bitumen and Peace River bitumen,[8])	1800	1374	6.54	1.9
asphaltenes (bitumens,[5,6,20−22])	1100	1274	6.84	1.75

molecular weight of asphaltenes is used because the association is introduced in the PR-EOS by treating the asphaltenes as aggregates of several molecules, considering that asphaltenes only interact with the rest of the mixture as an associated lump.

As the heavy component includes the aromatics and resins (and possibly heavy alkanes), the molecular weight M_w for the heavy component is estimated from the molar average values of aromatics and resins (and selected heavy alkanes) from the literature. After the molecular weights of all components are estimated, the molar average weight of bitumen is calculated and compared to that in the literature. The T_C, P_C, and ω for the heavy component are estimated from Cavett's correlation[23] and further adjusted to match the available experimental data in the literature.

In the CPA-EOS, the association parameters are ε_{AA}, ε_{AR}, κ_{AA}, κ_{AR}, N_A, and N_R. In line with the past work of Li and Firoozabadi,[13,14] we assume $N_A = N_R = 4$, $\kappa_{AA} = \kappa_{AR} = 0.01$ and $\varepsilon_{AA}/k_B = 2000K$. As a result, only the cross-association energy parameter between asphaltene and heavy molecules ε_{AR}, is adjusted. For each solvent, the cross-association parameter is obtained as follows. First, by changing the cross-association parameter as a model input, the range of cross-association parameters for which the model predicts different phase behavior than the experimental data is obtained. The analysis shows that the solubility of CO_2 and other alkanes in bitumens is usually not sensitive to the cross-association energy parameter in the CPA-EOS. Therefore, we keep the cross-association parameter constant at different temperatures for the same alkane−bitumen system. When there are two liquid phases with one having a high concentration of asphaltenes, then the results become sensitive to the cross-association energy parameter. The second liquid phase may have higher or lower asphaltene content than the first liquid phase. When the second liquid phase has significantly higher asphaltene content than the original bitumen, the CPA-EOS drastically improves phase behavior predictions when compared to the PR-EOS as we will discuss in various examples. In the following we investigate the phase behavior description of bitumen with CO_2 first and then discuss the results from methane to normal decane.

3.1. Athabasca Bitumen I/CO_2 System. Experimental data for the Athabasca bitumen I/CO_2 mixtures in vapor−liquid equilibrium are reported at temperatures from 293 to 353 K at saturation pressures between 20 and 120 bar.[20]

The SARA analysis of Athabasca bitumen I is provided in Table 2.[20] While the saturates are further characterized in terms of hydrocarbon cuts C_7, C_8, C_9, ..., C_{29} as in ref 20, we divide C_{30+} pseudocomponent into a heavy and asphaltene components based on the average molecular weight of the bitumen of 541 g/mol.[20] Table 3 provides the chemical composition of Athabasca bitumen I as well as the PR-EOS parameters and the binary interaction coefficients k_{ij} between CO_2 and other components, which are used in the calculations.

Table 2. SARA Analysis (wt %) of Several Bitumens[a]

	saturates	aromatics	resins	aromatics and resins	asphaltenes	solids
Athabasca bitumen I	17.2	24.1	38.6		20.1	0.0
Athabasca bitumen II	19.75			63.25	17.0	0.0
Athabasca bitumen III	19.5	47.0	17.1		16.1	0.3
Surmont bitumen	12.26	40.08	36.53		11.13	0.0
Athabasca vacuum tower bottoms	6.8	42.0	19.0		32.2	0.0
Peace River bitumen	18.5			62.0	19.3	0.2
Athabasca bitumen IV	17.0	46.9	16.7		19.4	0.0

[a]For Athabasca bitumens II and Peace River bitumen, only the combined amount of aromatics and resins is provided.

Table 3. Physical Parameters of Pseudocomponents and Composition for Athabasca Bitumen I[a]

component	wt (%)	T_C (K)	P_C (bar)	ω	M_w (g/mol)	$k_{i\text{-}C1}$ (−)	$k_{i\text{-}CO2}$ (−)
C_7	0.03	556.48	26.75	0.294	100	0.045	0.090
C_8	0.07	574.76	25.24	0.418	114	0.048	0.090
C_9	0.04	593.07	23.30	0.491	128	0.050	0.090
C_{10}	0.03	617.07	21.55	0.534	142	0.052	0.090
C_{11}	0.04	638.24	19.74	0.566	156	0.054	0.090
C_{12}	0.13	657.29	18.31	0.602	170	0.057	0.090
C_{13}	0.35	675.70	16.96	0.639	184	0.059	0.090
C_{14}	0.53	691.48	15.75	0.667	198	0.061	0.090
C_{15}	0.73	707.29	14.72	0.670	212	0.064	0.090
C_{16}	0.83	722.96	13.79	0.668	226	0.066	0.090
C_{17}	0.93	738.12	12.98	0.670	240	0.067	0.090
C_{18}	1.11	749.81	12.31	0.696	254	0.068	0.090
C_{19}	1.16	761.50	11.68	0.705	268	0.069	0.090
C_{20}	1.22	773.18	11.7	0.707	282	0.070	0.090
C_{21}	1.18	784.87	10.57	0.750	296	0.071	0.090
C_{22}	1.21	795.31	10.12	0.782	310	0.072	0.090
C_{23}	1.16	805.43	9.71	0.808	324	0.073	0.090
C_{24}	1.11	814.77	9.33	0.834	338	0.074	0.090
C_{25}	1.09	823.52	9.1	0.889	352	0.075	0.090
C_{26}	1.03	832.27	8.68	0.977	366	0.076	0.090
C_{27}	1.09	840.70	8.40	1.003	380	0.077	0.090
C_{28}	1.16	848.98	8.14	1.076	394	0.078	0.090
C_{29}	0.99	857.26	7.95	1.182	408	0.079	0.090
aromatics/resins	62.7	1033.81	6.95	1.460	600	0.080	0.092
asphaltenes	20.1	1274.0	6.84	1.750	1100	0.080	0.100

[a]This bitumen is mixed with CO_2 and C_1.

For mixtures of Athabasca bitumen I and CO_2, when the cross-association energy parameter between asphaltene and heavy molecules is less than 1200 K, instead of two-fluid phases, three-fluid phases are predicted. For values higher than 1200 K the solubility is predicted correctly. All of our results for CO_2 solubility are based on $\varepsilon_{AR}/k_B = 1200$ K.

In Figure 1, solubility of CO_2 in Athabasca bitumen I is presented vs pressure at four different temperatures (293, 313,
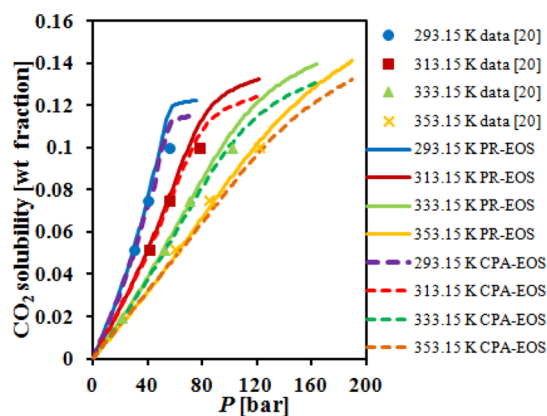

Figure 1. CO_2 solubility in Athabasca bitumen I vs pressure at different temperatures.

333, and 353 K). The CO_2 solubility in Athabasca bitumen I increases with increasing pressure at a given temperature and decreases with increasing temperature at a given pressure. Comparing the experimental data with the results obtained from the PR-EOS and CPA-EOS, the PR-EOS describes the overall trend, while the CPA-EOS slightly improves the calculations at higher pressures.

3.2. Athabasca Bitumen I/C_1 System. Data on mixtures of Athabasca bitumen I and methane (C_1) are also provided in ref 20 at temperatures from 293 to 353 K at saturation pressures between 29 and 162 bar. There is very little vaporization of bitumen components in the methane phase; thus, the molar fraction of methane in the bitumen-rich phase is the C_1 solubility.

The binary interaction coefficients k_{ij} between C_1 and other components are adjusted to match the experimental data given in ref 20. For mixtures of Athabasca bitumen I and C_1, when the cross-association energy parameter between asphaltene and heavy molecules is less than 1130 K, instead of two-fluid phases, three-fluid phases are predicted. For values higher than 1130 K the solubility is predicted correctly. All of our results for C_1 solubility are based on $\varepsilon_{AR}/k_B = 1130$ K.

In Figure 2, the solubility of C_1 in Athabasca bitumen I is presented vs pressure at four different temperatures (293, 313, 333, and 353 K). The C_1 solubility in Athabasca bitumen I increases with increasing pressure at constant temperature and decreases with increasing temperature at constant pressure. A comparison of Figures 1 and 2 shows that the solubility of CO_2 depends on temperature more strongly than the solubility of C_1. Both the PR-EOS and CPA-EOS provide predictions in line with experimental data.

3.3. Athabasca Bitumen II/C_2 System. For mixture of Athabasca bitumen II and C_2, experimental data in liquid–liquid equilibrium are reported with overall C_2 concentrations of 20, 40, 60, 80, and 90 wt % at ambient temperature at three different pressures (50, 70, and 90 bar).[21]

The Athabasca bitumen II composition is different from the composition of Athabasca bitumen I. SARA analysis for this bitumen is not reported; only the saturates, aromatics and resins (as one type of species), and asphaltenes are provided.
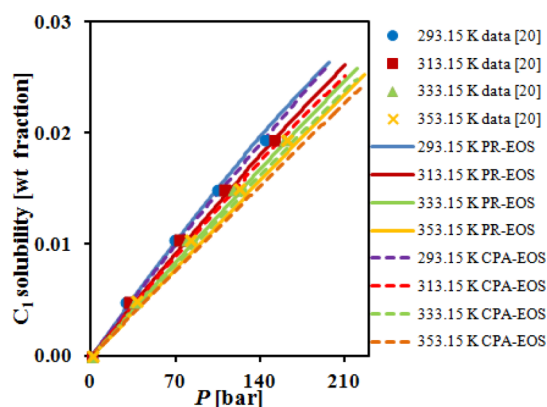
Figure 2. C_1 solubility in Athabasca bitumen I vs pressure at different temperatures.

The compositional analysis of Athabasca bitumen II is given in terms of 11 hydrocarbon cuts $C_4–C_{10}$, $C_{11}–C_{20}$, $C_{21}–C_{30}$, ..., $C_{90}–C_{100}$, C_{100+} in Figure 3 from ref 21. We have lumped these
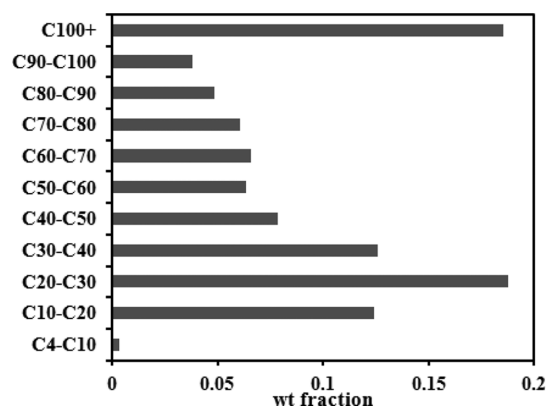

Figure 3. Compositional analysis of Athabasca bitumen II.[21]

cuts into five pseudocomponents for predictions. The saturates are characterized in terms of pseudocomponents $C_4–C_{10}$, $C_{11}–C_{20}$, and $C_{21}–C_{30}$. The rest of the hydrocarbon cuts from Figure 3 are lumped into heavy and asphaltene components. Molecular weight M_w of lighter pseudocomponents and heavy component are calculated as molar average values of relevant n-alkanes.[18] For asphaltenes, the molecular weight is assumed as 1100 g/mol.

Table 4 presents the compositional analysis of the bitumen together with the relevant EOS parameters. The values of T_C, P_C, and ω are estimated as molar average values of relevant n-alkanes from Cavett's correlation[23] and further adjusted to match the experimental data given in Tables 4 and 5. For mixtures of Athabasca bitumen II and C_2, when the cross-

Table 4. Physical Parameters of Pseudocomponents and Composition of Athabasca Bitumen II[a]

component	wt (%)	T_C (K)	P_C (bar)	ω	M_w (g/mol)
$C_4–C_{10}$	0.25	537.24	31.90	0.362	97.4
$C_{11}–C_{20}$	10.0	729.20	17.60	0.672	212.7
$C_{21}–C_{30}$	9.5	858.14	12.75	1.035	352.9
aromatics/resins	63.25	969.52	11.93	1.580	617.85
asphaltenes	17.0	1274.0	6.84	1.750	1100

[a]This bitumen is mixed with C_2.

association energy parameter between asphaltene and heavy molecules is less than 950 K, instead of two-fluid phases, three-fluid phases are predicted. For values higher than 950 K liquid–liquid states are predicted correctly. All of our results for C_2 calculations are based on $\varepsilon_{AR}/k_B = 950$ K.

In Tables 5 and 6, we present the experimental ethane composition in the ethane-rich phase (Liquid 1) and bitumen-rich phase (Liquid 2) for mixtures of Athabasca bitumen II and ethane at eight different conditions and the results from the PR-EOS and CPA-EOS. The calculation from the PR-EOS and CPA-EOS are in good agreement with experimental data. We also present the calculated asphaltene content in both phases in Tables 5 and 6. The asphaltene content in the lighter liquid phase is very low, while in the heavier liquid phase is approximately 14−19 wt %. As we will see later, when the asphaltene content of the asphaltene-rich liquid phase is high, the PR-EOS cannot predict reliable results.

3.4. Athabasca Bitumen III/C_3 System. Equilibrium experimental data for mixtures of Athabasca bitumen III and C_3 in two-phase are reported at temperatures varying from 283 to 323 K at pressures between 5 and 16 bar.[5]

Athabasca bitumen III has likely a different composition from Athabasca bitumens I and II. The SARA analysis of the bitumen is provided in Table 2[5] in which the fluid is characterized by six pseudocomponents. In this work, these pseudocomponents are replaced with saturates, heavy and asphaltene fractions based on the average molecular weight of bitumen of 552 g/mol.[5]

Table 7 lists the compositional analysis of the bitumen and the relevant EOS parameters. For mixtures of Athabasca bitumen III and C_3, when the cross-association energy parameter between asphaltene and heavy molecules is less than 970 K, instead of vapor–liquid states, liquid–liquid states, or three-fluid phases are predicted. For values higher than 970 K the solubility is predicted correctly and is not sensitive to the cross-association energy parameter in vapor–liquid equilibrium. However, when there are two liquid phases with one having a high concentration of asphaltenes, then the results become sensitive to the cross-association energy parameter. All of our results for C_3 calculations are based on $\varepsilon_{AR}/k_B = 970$ K.

Solubility of propane in bitumen strongly depends on whether the propane-rich phase is liquid or gas at conditions of measurement. We calculate saturation pressure when a small amount of the second phase appears. The modeling results show that the second phase may be vapor at lower pressures and a heavy liquid phase at higher pressures depending on the temperature in line with the saturation pressure of pure propane in the NIST database.[24] In Figure 4, the solubility data from ref 5 and the EOS results are plotted as functions of pressure showing the effect of temperature on C_3 solubility in the bitumen-rich phase in Athabasca bitumen III. In Figure 5, the corresponding predicted asphaltene content in the bitumen-rich phase is plotted from the PR-EOS and CPA-EOS. These two figures show that C_3 solubility in Athabasca bitumen III increases with increasing pressure at a given temperature and decreases with increasing temperature at a given pressure, and the asphaltene content in the bitumen-rich phase decreases with increasing pressure at a given temperature and increases with increasing temperature at a given pressure.

In Figure 6, the solubility of C_3 in the second phase is presented vs pressure at five different temperatures (283, 293, 303, 313, and 323 K). In Figure 7, the corresponding predicted asphaltene content in the second phase is plotted for the PR-EOS and CPA-EOS.

Table 5. Liquid−Liquid Equilibrium Data (Ethane and Asphaltene Contents in the Ethane-Rich Liquid Phase L₁) of the Mixture of Athabasca Bitumen II and C₂ at Ambient Temperatures and Different Pressures[21]
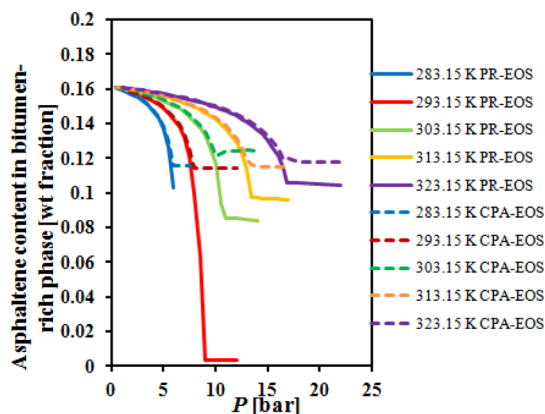
			C_2 content in L_1 (wt frac)			asphaltene content in L_1 (wt frac)	
P (bar)	T (K)	C_2 in feed (wt %)	data	PR	CPA	PR	CPA
50.9	295.9	20		0.8995	0.8357	1.10×10^{-4}	2.7312×10^{-6}
50.8	294.8	40	0.9140	0.9224	0.8972	7.68×10^{-5}	6.8212×10^{-7}
50.5	294.7	60	0.9290	0.9476	0.9378	3.68×10^{-5}	1.8319×10^{-7}
70.8	294.7	40	0.8770	0.8912	0.8635	6.56×10^{-4}	4.6354×10^{-6}
90.8	294.6	40	0.8450	0.8677	0.8403	2.18×10^{-3}	1.4028×10^{-5}
90.8	294.3	60	0.8900	0.9168	0.9077	1.24×10^{-3}	5.189×10^{-6}
90.4	294.7	80	0.9310	0.9776	0.9564	5.25×10^{-4}	2.1325×10^{-6}
90.5	294.3	90	0.9600	0.9774	0.9772	5.62×10^{-4}	1.5288×10^{-6}

Table 6. Liquid−Liquid Equilibrium Data (Ethane and Asphaltene Content in the Bitumen-Rich Liquid Phase L₂) of the Mixture of Athabasca Bitumen II and C₂ at Ambient Temperatures and Different Pressures[21]

			C_2 content in L_2 (wt frac)			asphaltene content in L_2 (wt frac)	
P (bar)	T (K)	C_2 in feed (wt %)	data	PR	CPA	PR	CPA
50.9	295.9	20	0.1790	0.1763	0.1556	0.1405	0.1454
50.8	294.8	40	0.1570	0.1666	0.1446	0.1474	0.1542
50.5	294.7	60	0.1450	0.1548	0.1342	0.1549	0.1616
70.8	294.7	40	0.1660	0.1789	0.1510	0.1475	0.1566
90.8	294.6	40	0.1660	0.1926	0.1588	0.1461	0.1577
90.8	294.3	60	0.1550	0.1751	0.1464	0.1574	0.1681
90.4	294.7	80	0.1310	0.1493	0.1343	0.1762	0.1786
90.5	294.3	90	0.1160	0.1500	0.1289	0.1761	0.1866

Table 7. Parameters of Pseudocomponents and Composition of the Mixture of Athabasca Bitumen III and C₃ or nC₇

component	wt (%)	T_C (K)	P_C (bar)	ω	M_w (g/mol)
saturates	19.5	930	11.98	0.9	460
aromatics/resins	64.1	1074	10.85	1.5	660
asphaltenes	16.4	1274	6.84	1.75	1100
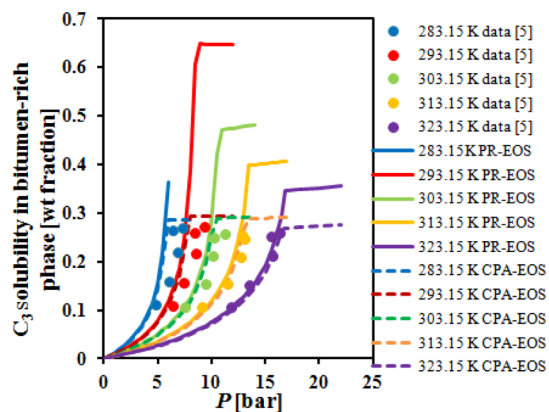
Figure 4. Solubility of C_3 in the bitumen-rich phase of Athabasca bitumen III vs pressure at different temperatures.

Figure 5. Asphaltene content in the bitumen-rich phase of Athabasca bitumen III vs pressure at different temperatures.

The results from the PR-EOS and CPA-EOS are in good agreement with data when the new phase is vapor. At higher pressures when the second liquid phase appears, the PR-EOS becomes inaccurate; it predicts a single liquid phase at the temperature of 283 K and pressures higher than 6 bar, at higher temperatures the second liquid phase is detected but is not described correctly. Similarly, the asphaltene contents in both liquid phases are predicted inaccurately from the PR-EOS. As can be seen from Figure 5, the asphaltene content in the

bitumen-rich phase predicted using the CPA-EOS is approximately 11 wt % for all temperatures from 283 to 323 K. For temperatures lower than 303 K, the asphaltene content in the second liquid phase from the CPA-EOS is higher than that in the bitumen-rich phase (up to 16 wt %). For temperatures higher than 303 K, the asphaltene content in the second phase is almost zero. The results show that the CPA-EOS describes the C_3 solubility in the bitumen correctly when a second liquid phase appears. All of the results above pertain to the conditions when the amount of the second phase is small.

3.5. Surmont Bitumen/nC₄ System. Experimental data for mixtures of Surmont bitumen and nC_4 in vapor−liquid equilibrium are available over a wide range of temperature (373, 423, 448, and 463 K) at pressures from 8 to 60 bar.[22]

The SARA analysis of Surmont bitumen is provided in Table 2.[22] The bitumen is characterized using several pure components, saturates, heavy and asphaltene components
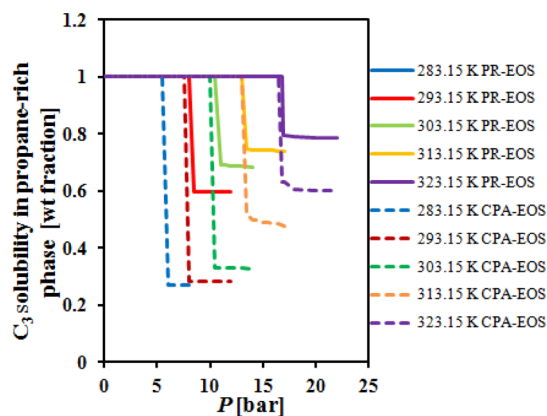
Figure 6. C_3 content in the C_3-rich phase of Athabasca bitumen III vs pressure at different temperatures. The amount of the phase is very small.
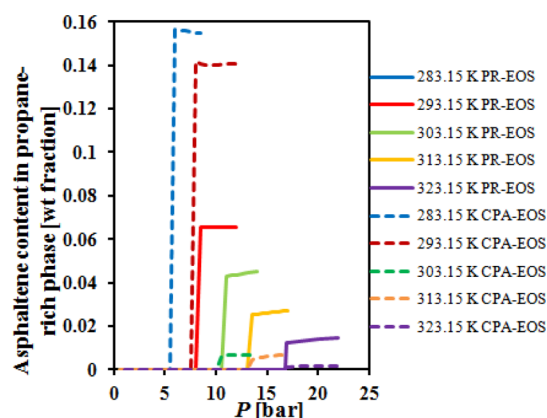

Figure 7. Asphaltene content in the C_3-rich phase of Athabasca bitumen III vs pressure at different temperatures.

based on the average molecular weight of the bitumen of 539.2 ± 7.9 g/mol from ref 22. The EOS parameters for bitumen pseudocomponents are listed in Table 8. For mixtures of the bitumen and nC_4, when the cross-association energy parameter between asphaltene and heavy molecules is less than 500 K, instead of two-fluid phases, three-fluid phases are predicted. For values higher than 500 K the solubility is predicted correctly.

Table 8. Parameters of Pseudocomponents and Composition of Surmont Bitumen[a]

component	wt (%)	T_C (K)	P_C (bar)	ω	M_w (g/mol)
C_7	0.058	556.48	26.75	0.294	100
C_8	0.063	574.76	25.24	0.418	114
C_9	0.065	593.07	23.30	0.491	128
C_{10}	0.081	617.07	21.55	0.534	142
C_{11}	0.125	638.24	19.74	0.566	156
C_{12}	0.513	657.29	18.31	0.602	170
C_{13}	0.927	675.70	16.96	0.639	184
C_{14}	1.346	691.48	15.75	0.667	198
C_{15}	1.822	707.29	14.72	0.670	212
saturates	7.26	868.89	11.85	1.280	407
aromatics/resins	76.61	933.81	10.83	1.670	573
asphaltenes	11.13	1274.00	6.84	1.750	1100

[a]The bitumen is mixed with nC_4 and nC_5.

All of our results for nC_4 calculations are based on $\varepsilon_{AR}/k_B = 1000$ K.

In Figure 8, we present the effect of temperature on nC_4 solubility in the liquid phase for mixtures of Surmont bitumen
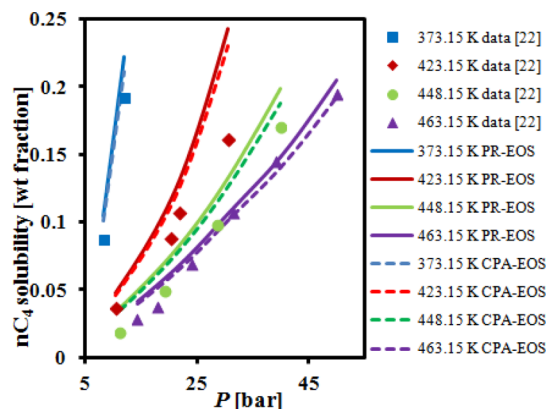

Figure 8. Solubility of nC_4 in Surmont bitumen vs pressure at different temperatures.

and nC_4 at different pressures. The results from the PR-EOS and CPA-EOS are in good agreement with the experimental data indicating that the PR-EOS describes the phase behavior of the system well. In addition, Figure 8 shows that nC_4 solubility in Surmont bitumen increases with increasing pressure at a given temperature and decreases with increasing temperature at a given pressure. Comparing the solubility plots of nC_4, where there is a distinct difference between the isotherms (see Figure 8) with CO_2 or C_1, where the isotherms are close to each other (see Figure 1 and Figure 2), it can be seen that nC_4 has much higher solubility in bitumen than CO_2 and lighter hydrocarbons at the same conditions. The solubility of nC_4 in the bitumen at high temperatures (e.g., 463 K) is significantly higher than C_3 solubility whose solubility is appreciable at lower temperature conditions, while by increasing the temperature, the solubility is substantially reduced.

3.6. Surmont Bitumen/nC_5 System. Experimental data for mixtures of Surmont bitumen and normal pentane (nC_5) in vapor−liquid equilibrium are provided in ref 22 at the temperature of 422 K at pressures from 8 to 15 bar.

We use the same EOS parameters for the Surmont bitumen and nC_5 mixture as in nC_4. For mixtures of Surmont bitumen and nC_5, when the cross-association energy parameter between asphaltene and heavy molecules is less than 900 K, instead of two-fluid phases, three-fluid phases are predicted. For values higher than 900 K the solubility is predicted correctly. All of our results for nC_5 calculations are based on $\varepsilon_{AR}/k_B = 1050$ K.

In Figure 9, the solubility of nC_5 in Surmont bitumen is presented as a function of pressure at the temperature of 422 K. The nC_5 solubility in Surmont bitumen increases with increasing pressure at a given temperature and decreases with increasing temperature at a given pressure. The agreement between the PR-EOS and CPA-EOS and measured data is not as good as for the other mixtures.

3.7. Athabasca Bitumen III/C_3, nC_7 Systems. Experimental data for mixtures of Athabasca bitumen III and C_3 in two-phase equilibrium are reported at temperatures ranging from 283 to 333 K at pressures from 3 to 16 bar.[6] The asphaltene yields from the n-heptane-diluted Athabasca bitumen III at ambient conditions are also reported in ref 6. The
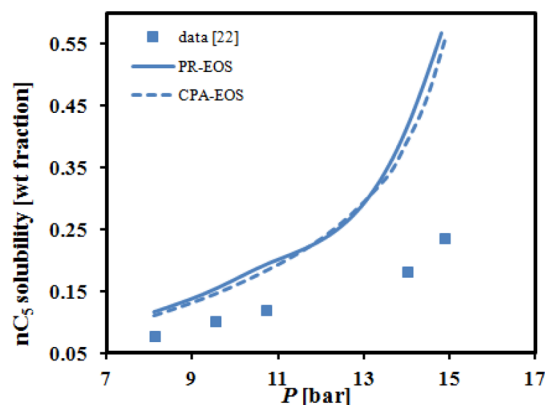
Figure 9. Solubility of nC_5 in Surmont bitumen vs pressure at 422 K.

fractional yield of asphaltene precipitation from bitumen is defined as the mass of precipitated asphaltenes and solids divided by the mass of the heavy oil or bitumen.

The SARA analysis of Athabasca bitumen III is provided in Table 2.[6] The "solids" are assumed to precipitate directly and, therefore, are not included in the phase-split calculations. The EOS parameters for Athabasca bitumen III and C_3 and nC_7 mixtures are listed in Table 7. For mixtures of Athabasca bitumen III and C_3, we use the same cross-association energy parameter between asphaltene and heavy molecules as in Section 3.3, that is, $\varepsilon_{AR}/k_B = 970$ K. For mixture of Athabasca bitumen III and nC_7, asphaltene yield is very sensitive to the cross-association energy parameter between asphaltene and heavy molecules. All of our results for nC_7 calculations are based on $\varepsilon_{AR}/k_B = 1250$ K.

In Figure 10, data from ref 6 and the EOS results are plotted in the $P-T$ diagram for different overall amounts of C_3 diluted
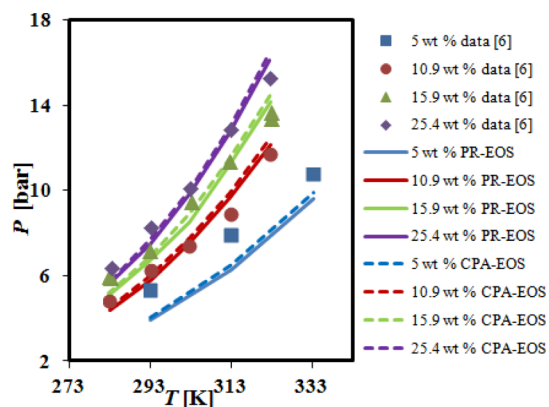

Figure 10. $P-T$ diagram for different overall amounts of C_3 diluted in Athabasca bitumen III.

in Athabasca bitumen III. The figure shows that pressure increases with increasing temperature for a given overall amount of C_3 diluted in the bitumen and increases with increasing overall amount of C_3 diluted in the bitumen at a given temperature. The results from the PR-EOS and CPA-EOS are in good agreement with experimental data for vapor–liquid states except for the lowest overall amount of C_3 where the agreement between predictions and measurements is poor. The results are also comparable to modeling results from ref 6 using the PR-EOS with modifications (as described in the introduction).

In Figure 11, the experimental and calculated asphaltene and solid fractional yields are presented for Athabasca bitumen III
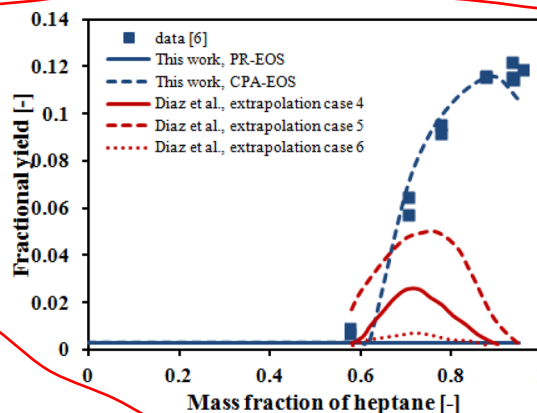

Figure 11. Asphaltene fractional yield vs n-heptane amount for Athabasca bitumen III at 296.15 K and 0.9 bar.

mixed with nC_7 at 296.15 K and 0.9 bar and compared with the modeling results from ref 6. As can be seen from the figure, a single liquid phase is predicted using the PR-EOS regardless of the amount of nC_7 mixed with the bitumen. In contrast, the CPA-EOS describes the phase behavior of mixtures of bitumens and nC_7 in liquid–liquid states, and the results are in good agreement with the experimental data. The modeling results from ref 6 using the modified PR-EOS cannot correctly predict asphaltene yields from n-heptane diluted bitumen. When increasing the overall mass fraction of nC_7 from approximately 70 to 95 wt %, the corresponding asphaltene content in the bitumen-rich liquid phase is very low (lower than 2 wt %), while the asphaltene content in the second liquid phase increases from approximately 21 to 54 wt %. The high asphaltene content results in significant association and cross-association described by the CPA-EOS.

3.8. Athabasca Vacuum Tower Bottoms/nC_{10} Systems. Experimental data for mixtures of the Athabasca vacuum tower bottoms (AVTB) and nC_{10} in vapor–liquid and vapor–liquid–liquid equilibrium are reported at temperatures ranging from 315 to 615 K at pressures up to 16 bar.[7] AVTB are the heaviest parts of bitumen containing 32 wt % of asphaltenes.

The SARA analysis of AVTB is provided in Table 2[7] where the authors characterized the fluid using 20 pseudocomponents. In this work, these pseudocomponents are replaced with saturates, heavy and asphaltene fractions. The EOS parameters for AVTB and nC_{10} mixtures are listed in Table 9. For mixtures of AVTB and nC_{10}, when the cross-association energy parameter between asphaltene and heavy molecules is less than 900 K, instead of vapor–liquid states, liquid–liquid states are predicted. For values higher than 900 K vapor–liquid and vapor–liquid–liquid states are predicted correctly. Our results are based on $\varepsilon_{AR}/k_B = 1200$ K.

Table 9. Parameters of Pseudocomponents and Composition of the Athabasca Vacuum Tower Bottoms[a]

component	wt (%)	T_C (K)	P_C (bar)	ω	M_w (g/mol)
saturates	6.8	990	9.6	0.15	446
aromatics/resins	61.0	1086	8.05	1.75	765
asphaltenes	32.2	1522	6.17	2.0	3730

[a]The bitumen is mixed with nC_{10}.

In Figure 12, data from ref 7 and the EOS results are plotted in the $P-T$ diagram for two different overall amounts of nC_{10}
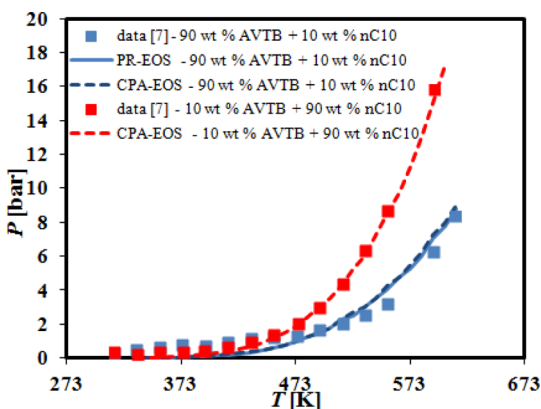

Figure 12. Saturation pressure vs temperature for mixture of the Athabasca vacuum tower bottoms and nC_{10}.

(10 and 90 wt %) diluted in AVTB. When 10 wt % of nC_{10} is mixed with 90 wt % of AVTB, a small amount of a vapor phase appears at the saturation pressure at the given temperature. The results from the PR-EOS and CPA-EOS are in good agreement with experimental data and are also comparable to modeling results from[7] using the PR-EOS with the proposed mixing rules. When 90 wt % of nC_{10} is mixed with 10 wt % of AVTB, liquid–liquid states are observed with a small amount of a vapor phase which appears at the specific pressure and temperature. The results from the CPA-EOS are in good agreement with experimental data while both the PR-EOS and the calculation from ref 7 do not predict the second liquid phase.

3.9. Athabasca IV and Peace River Bitumens/CO_2, nC_5 Systems. Experimental data for mixtures of Peace River bitumen and CO_2 in two-phase equilibrium are reported at temperatures ranging from 296 to 378 K at pressures from 15 to 62 bar.[8] The asphaltene yields are also reported for the n-pentane diluted Athabasca bitumen IV at ambient conditions.[8]

The SARA analyses of Athabasca bitumen IV and Peace River bitumen are provided in Table 2.[8] The "solids" are assumed to precipitate directly and, therefore, are not included in the phase-split calculations. In ref 8, the bitumens are characterized using 16 pseudocomponents. In this work, these pseudocomponents are replaced with saturates, heavy and asphaltene fractions. The EOS parameters for the Athabasca bitumen IV and nC_7 mixtures and Peace River bitumen and CO_2 mixtures are listed in Table 10 including binary interaction coefficients k_{ij} between CO_2 and other components, which are used in the calculations. For mixtures of Athabasca bitumen IV and nC_5, asphaltene yield is very sensitive to the cross-association energy parameter between asphaltene and heavy molecules. All of our results for nC_5 calculations are based on $\varepsilon_{AR}/k_B = 1300$ K. For mixtures of Peace River bitumen and CO_2, the solubility of CO_2 in the bitumen is not sensitive to the

cross-association energy parameter; therefore, we use the same cross-association energy parameter between asphaltene and heavy molecules as for nC_5.

In Figure 13, the solubility of CO_2 in Peace River bitumen is presented vs pressure at five different temperatures (296, 310,
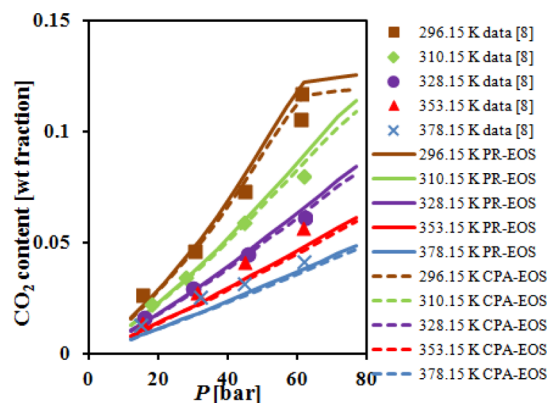

Figure 13. Solubility of CO_2 in Peace River bitumen vs pressure at different temperatures.

328, 353, and 378 K). CO_2 solubility in Peace River bitumen increases with increasing pressure at a given temperature and decreases with increasing temperature at a given pressure. At the temperature of 296 K and pressures higher than 60 bar, a small amount of a second liquid appears, and the solubility in the bitumen-rich phase predicted from the CPA-EOS is constant with increasing pressure. The results from the PR-EOS and CPA-EOS are in good agreement with experimental data for vapor–liquid states and are also comparable to modeling results from[8] using the PR-EOS and temperature-dependent binary interaction coefficients.

In Figure 14, the experimental and calculated asphaltene and solid fractional yields are presented for Athabasca bitumen IV
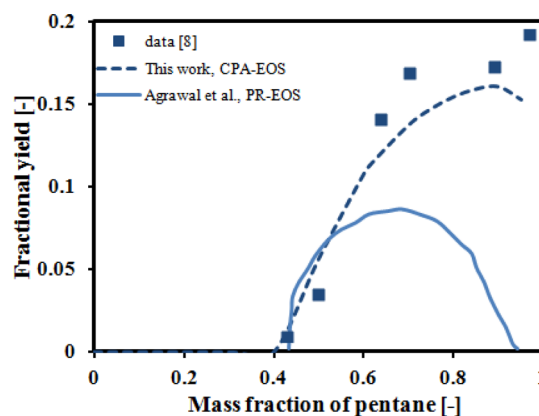

Figure 14. Asphaltene fractional yield vs n-pentane amount for Athabasca bitumen IV at 296.15 K and 1 bar.

Table 10. Composition and Parameters of Pseudocomponents of Athabasca Bitumen IV and Peace River Bitumen[a]

component	wt (Athabasca bitumen IV) (%)	wt (Peace River bitumen) (%)	T_C (K)	P_C (bar)	ω	M_w (g/mol)	$k_{i\text{-}CO_2}$ (−)
saturates	17.0	18.5	823.5	13.0	0.8	323	0.09
aromatics/resins	63.6	62.0	953	7.88	1.28	589	0.09
asphaltenes	19.4	19.3	1374	6.54	1.9	1800	0.1

[a]Athabasca bitumen IV is mixed with nC_5, and Peace River bitumen is mixed with CO_2.

mixed with nC_5 at 296.15 K and 1 bar and compared with the modeling results from ref 8. The PR-EOS predicts a single liquid phase regardless of the amount of nC_5 mixed with the bitumen. In contrast, the CPA-EOS describes the phase behavior of mixtures of bitumens and nC_5 in liquid–liquid states, and the results are in good agreement with the experimental data. The modeling results in ref 8 from the PR-EOS and temperature-dependent binary interaction coefficients do not describe asphaltene yields from the n-pentane diluted bitumen. When increasing the overall mass fraction of nC_5 from approximately 50 to 95 wt %, the corresponding asphaltene content in the bitumen-rich liquid phase is very low (lower than 8 wt %), while the asphaltene content in the second liquid phase increases from approximately 75 to 82 wt %. The high asphaltene content results in significant association and cross-association described by the CPA-EOS.

4. SUMMARY AND CONCLUSIONS

We present the results from the Peng–Robinson and cubic-plus-association equations of state to model the solubility and phase behavior of CO_2 and light alkanes (C_1 to nC_{10}) in several bitumens. Bitumens are characterized by three or more pseudocomponents including saturates, aromatics/resins, and asphaltenes. The component which is mixed with bitumen is represented fully. The parameters of the CPA-EOS for all the pseudocomponents are mostly taken from the literature (N_A, N_R, ε_{AA}, κ_{AA}, and κ_{AR}, T_C, P_C, ω, and M_w). As a result, only the cross-association energy between asphaltene and aromatic/resin molecules ε_{AR} remains to be determined. In this work, we show that the solubility of CO_2 and other alkanes in bitumens is not sensitive to this parameter in the CPA-EOS with the exception of systems with two liquid phases with one having a high concentration of asphaltenes. The CPA-EOS results then become sensitive to the cross-association energy parameter.

We apply the PR-EOS and CPA-EOS and reproduce experimental data of phase behavior and solubilities of CO_2 and alkanes in bitumens over a wide range of temperature and pressure. In vapor–liquid equilibrium, we predict the phase behavior of bitumens mixed with CO_2, C_1, C_3, nC_4, nC_5, and nC_{10}. The results from the PR-EOS and CPA-EOS are in good agreement indicating that the PR-EOS predicts the solubilities in the liquid phase well. Therefore, there is no need to take the association into account. The PR-EOS describes the phase behavior of mixtures of bitumens and alkanes in liquid–liquid states for which the asphaltene content in the liquid phase is low (as in case of C_2). However, in liquid–liquid states where the asphaltene content of one of the phases is high resulting in significant association and cross-association, the PR-EOS does not work well. The CPA-EOS works well for such systems.

■ AUTHOR INFORMATION

Corresponding Authors
*Telephone: +420-224-358553. E-mail: jiri.mikyska@fjfi.cvut.cz.
*E-mail: abbas.firoozabadi@yale.edu.

Notes
The authors declare no competing financial interest.

■ ACKNOWLEDGMENTS

■ REFERENCES

(1) Zou, X.; Zhang, X.; Shaw, J. Phase Behavior of Athabasca Vacuum Bottoms + n-Alkane Mixtures. *SPE Production & Operations* **2007**, *22*, 265–272.

(2) Prausnitz, J. M.; Lichtenthaler, R. N.; de Azevedo, E. G. *Molecular Thermodynamics of Fluid-Phase Equilibria*; Prentice-Hall, 1999.

(3) Zirrahi, M.; Hassanzadeh, H.; Abedi, J.; Moshfeghian, M. Prediction of Solubility of CH4, C2H6, CO2, N2 And CO in Bitumen. *Can. J. Chem. Eng.* **2014**, *92*, 563–572.

(4) Rezaei, N.; Mohammadzadeh, O.; Chatzis, I. Warm VAPEX: A Thermally Improved Vapor Extraction Process for Recovery of Heavy Oil and Bitumen. *Energy Fuels* **2010**, *24*, 5934–5946.

(5) Nourozieh, H.; Kariznovi, M.; Abedi, J. Investigation of Different Models for Thermodynamic Modeling of Bitumen/Propane Mixture. *Can. Energy Technol. & Innovation* **2012**, *1*, 33–40.

(6) Díaz, O.; Modaresghazani, J.; Satyro, M.; Yarranton, H. Modeling the Phase Behavior of Heavy Oil and Solvent Mixtures. *Fluid Phase Equilib.* **2011**, *304*, 74–85.

(7) McFarlane, R.; Gray, M.; Shaw, J. Evaluation of Co-volume Mixing Rules for Bitumen Liquid Density and Bubble Pressure Estimation. *Fluid Phase Equilib.* **2010**, *293*, 87–100.

(8) Agrawal, P.; Schoeggl, F. F.; Satyro, M. A.; Taylor, S. D.; Yarranton, H. W. Measurement and Modeling of the Phase Behavior of Solvent Diluted Bitumens. *Fluid Phase Equilib.* **2012**, *334*, 51–64.

(9) Sabbagh, O.; Akbarzadeh, K.; Badamchi-Zadeh, A.; Svrcek, W. Y.; Yarranton, H. W. Applying the PR-EoS to Asphaltene Precipitation from n-Alkane Diluted Heavy Oils and Bitumens. *Energy Fuels* **2006**, *20*, 625–634.

(10) Wu, J.; Prausnitz, J. M.; Firoozabadi, A. Molecular-Thermodynamic Framework for Asphaltene-Oil Equilibria. *AIChE J.* **1998**, *44*, 1188–1199.

(11) Ting, P. D.; Hirasaki, G. J.; Chapman, W. G. Modeling of Asphaltene Phase Behavior with the SAFT Equation of State. *Pet. Sci. Technol.* **2003**, *21*, 647–661.

(12) Huang, S. H.; Radosz, M. Phase Behavior of Reservoir Fluids V: SAFT Model of CO2 and Bitumen Systems. *Fluid Phase Equilib.* **1991**, *70*, 33–54.

(13) Li, Z.; Firoozabadi, A. Cubic-Plus-Association Equation of State for Asphaltene Precipitation in Live Oils. *Energy Fuels* **2010**, *24*, 2956–2963.

(14) Li, Z.; Firoozabadi, A. Modeling Asphaltene Precipitation by n-Alkanes from Heavy Oils and Bitumens Using Cubic-Plus-Association Equation of State. *Energy Fuels* **2010**, *24*, 1106–1113.

(15) Zirrahi, M.; Hassanzadeh, H.; Abedi, J. Prediction of CO2 Solubility in Bitumen Using a Cubic-Plus-Association Equation of State (CPA-EoS). *J. Supercrit. Fluids* **2015**, *98*, 44–49.

(16) Peng, D. Y.; Robinson, D. B. A New Two-Constant Equation of State. *Ind. Eng. Chem. Fundam.* **1976**, *15*, 59–64.

(17) Peng, D. Y.; Robinson, D. B.; Chung, S. Y. K. The Development of the Peng-Robinson Equation and Its Application to Phase Equilibrium in a System Containing Methanol. *Fluid Phase Equilib.* **1985**, *24*, 25–41.

(18) Firoozabadi, A. *Thermodynamics and Applications in Hydrocarbon Energy Production*; McGraw-Hill: New York, 2015.

(19) Kontogeorgis, G. M.; Voutsas, E. C.; Yakoumis, I. V.; Tassios, D. P. An Equation of State for Associating Fluids. *Ind. Eng. Chem. Res.* **1996**, *35*, 4310–4318.

(20) Varet, G.; Montel, F.; Nasri, D.; Daridon, J.-L. Gas Solubility Measurement in Heavy Oil and Extra Heavy Oil at Vapor Extraction (VAPEX) Conditions. *Energy Fuels* **2013**, *27*, 2528–2535.

(21) Nourozieh, H.; Kariznovi, M.; Abedi, J. Physical Properties and Extraction Measurements for the Athabasca Bitumen+Light Hydrocarbon System: Evaluation of the Pressure Effect, Solvent-to-Bitumen Ratio, and Solvent Type. *J. Chem. Eng. Data* **2011**, *56*, 4261–4267.

(22) Kariznovi, M. *Phase Behaviour Study and Physical Properties Measurement for Athabasca Bitumen/Solvent Systems Applicable for*

Thermal and Hybrid Solvent Recovery Processes. Ph.D. thesis, University of Calgary, 2013.

(23) Cavett, R. H. Physical Data for Distillation Calculations, Vapor-Liquid Equilibria. In *Proceeding of 27th API Meeting*; API Division of Refining: San Francisco, 1962.

(24) Lemmon, E. W.; McLinden, M. O.; Friend, D. G. *Thermophysical Properties of Fluid Systems*; National Institute of Standards and Technology; http://webbook.nist.gov/chemistry/.